# NEAR INFRARED IMAGING AND SPECTROSCOPY FOR BRAIN ACTIVITY MONITORING

Il-Young Son, Birsen Yazıcı
*Rensselaer Polytechnic Institute*
*Troy, NY 12180, USA*

**Abstract**   The first demonstration that near infrared (NIR) light can be used to monitor the state of cortical tissues noninvasively through the skull was presented by Jobsis in 1977 [53]. About a decade later, researchers started looking at the potential use of NIR spectroscopy for functional brain activity monitoring. Early studies began with simple motor and sensory tasks demonstrating the feasibility of the technology for noninvasively assessing the state of cerebral activity in a localized area. More recent studies have attempted to monitor more complex cognitive tasks such as warfare management [48] and aircraft landing simulations [102]. In this chapter, the research surrounding the application of NIR imaging and spectroscopy to noninvasive monitoring of functional brain activity is reviewed. A comprehensive review of equipment technologies, mathematical models, and past studies is given with some emphasis on the techology's potential in security and defense applications.

**Keywords:**   functional brain monitoring; near infrared spectroscopy; diffuse optical tomography

## 1.     Introduction

Near infrared imaging and spectroscopy is an emerging technology concerned with monitoring the changes in the state of biological tissues using light in the range of 600 to 900 nm. The optical properties of the major chromophores within this range makes NIR especially attractive for tissue imaging. The plausibility of using NIR to noninvasively monitor the state of cortical tissue was first demonstrated almost 30 years ago by F. F. Jobsis in his seminal paper, "Noninvasive, infrared monitoring of cerebral and myocardial oxygen sufficiency and circulatory parameter" [53]. He was the first to show that it was possible to penetrate the skull using near infrared light as the source. It would take another

decade before advances in technology allowed non-invasive monitoring of brain function using NIR methods. Some of the first demonstrations of brain activity monitoring were performed by Chance et. al. [12], Hoshi et. al. [46] and Villringer et. al. [109].

The research into NIR based brain activity monitoring was motivated by its potential as an alternative to older and more established imaging modalities such as functional magnetic resonance imaging (fMRI) and positron emission tomography (PET). There are several motivating factors for researching the potential of NIR based methods. For one, the NIR method provides information about physiological parameters not available in other modalities, such as oxygenation information. Secondly, NIR equipment has higher temporal resolution, in the order of milliseconds, compared to fMRI and PET [52]. This allows for, among other things, being able to model fast oscillatory noise related to normal physiological functions [34]. Thirdly, NIR equipment is relatively less restraining compared to fMRI or PET and generally safer than PET as it does not rely on ionizing radiation. Some types of NIR equipment, namely those using continuous wave signals, has also been made portable and in some instances, telemetric [11, 45].

With these motivations as a driving force, the research into NIR based brain activity monitoring have blossomed in the past 20 years with growing number of potential applications. So far, brain activity monitoring has seen applications in physiological studies of brain disfunction, preterm neonatal care, education and training, and cognitive workload assessment.

The list is not exhaustive but gives some idea of the variety of fields in which it finds utility. Workload assessment is particularly of interest to security and defense research. The DARPA's Augmented Cognition (AugCog) program, for example, have used EEG's, NIR, and fMRI technologies to monitor cerebral responses to a given complex cognitive task. The goal of such *operator monitoring* is to assess the cognitive state of the operator and adapt the system accordingly to mitigate the effect of information processing bottleneck in order to optimize his or her performance output. The assumption is that by noninvasively monitoring cerebral response to varying task conditions, it may be possible to extract patterns and infer the cognitive state of the task performer. Additionally, it has potential applications in emergency medicine in battle field, and operator fatigue assessment in stressful environments.

In this review, it is our goal to give an overview of the breadth of research conducted in the past 20 years. As with most review of this nature, we cover the breadth and do not intend to provide close in depth

survey of all the research available in this area. However, we provide a comprehensive review and point to motivations for further research.

With these goals in mind, we structured the chapter as follows: First, an overview of the types of imaging system used in NIR spectroscopy studies is given. This is followed by sections describing in some detail the two different kinds of signals that NIR method can measure. The two types of signals are characterized by their response time, namely fast response and slow response signals. The fast signal is associated with changes in neuronal tissue and slow signal is related to changes in the state of hemoglobin concentration and oxygenation (hemodynamics). The fast signal have latency of around 50 to 300 ms and slow signal have latency of about 10 seconds [32]. Lastly, an overview of human studies with an emphasis on security and defense applications is given. This is followed by some closing remarks on the future direction of research.

## 2.     NIR Imaging and Spectroscopy Systems

Three types of light sources have been suggested for use in NIR imaging and spectroscopy systems [11, 7]. The simplest of these are continuous wave (CW) sources. As such most commercially available systems use CW light as their source [44]. CW-type instruments are able to assess regional cerebral blood flow by measuring light attenuation through the cortical tissue and calculating their hemodynamic responses, i.e. changes in hemoglobin concentration and oxygenation, using these attenuation measurements. With these absorption measurements, however, it is very difficult, if not impossible, to gauge the absolute concentration changes since the real path length of light photons are unknown and cannot be measured or inferred. CW-type instruments rely on simplified assumptions about the nature of the media being probed and the changes occurring inside the sampling volume. As such, only relative concentration changes from some baseline measurement can be assessed. The advantage of using a CW-type instrument is that they are inexpensive and can be made portable. An example of CW-type system used in our lab is pictured in figure 1. As can be seen from the figure the entire system is quite compact. The probe itself is highly flexible, thus relatively comfortable to wear and consists of array of photosensors and diodes. A close-up of the probe is pictured in figure 2.

In order to better quantify the absolute value of chromophore concentrations, time of flight (TOF) must be measured in addition to light attenuation. This may be achieved using time-resolved or frequency domain methods. Time-resolved spectroscopy (TRS) was first pioneered by Delpy et. al. [19], Patterson et. al. [85] and Chance et al. [12, 13].
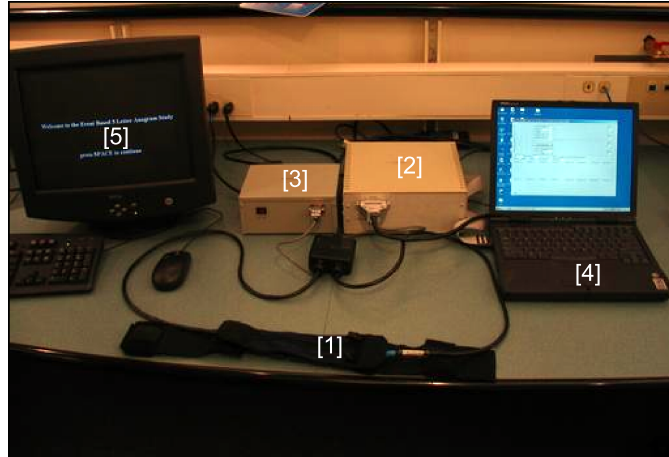
*Figure 1.* An example of CW-type system: 1. probe 2. data processing unit for pre-filtering and managing control signals 3. power supply 4. laptop computer for recording data and sending control signals to the probe 5. computer for hosting the task
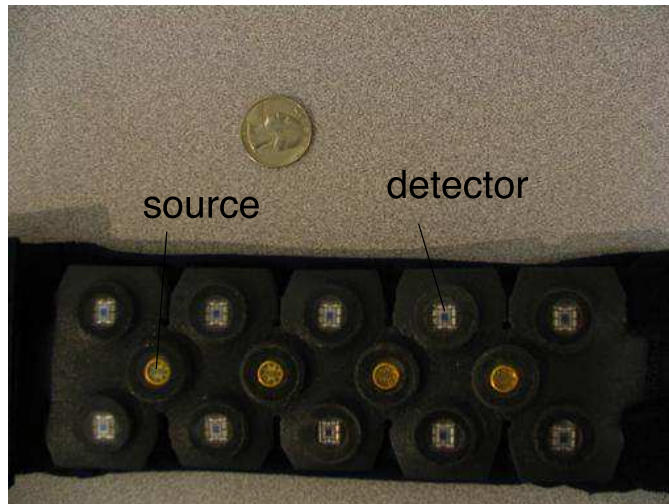


*Figure 2.* Close of the probe used in our laboratory. The quarter is for size reference.

Since then, number of researcher have studied and experimented with TRS including Chance and Oda [61, 63, 76, 80, 81, 73, 82, 113, 114]. TRS instruments rely on a picosecond pulsed laser with a detector that is designed to detect the time evolution of the light intensity [44]. With the time profile of light intensity through the medium, it is possible to measure both absorption and reduced scattering coefficients [32]. A ma-

jor draw back of TRS instruments is that they are relatively expensive. For this reason, these instruments have mostly been built for research purposes and are not readily available commercially.

Frequency domain method was first suggested by Gratton et. al. in [31]. Frequency domain approach uses radio frequency intensity modulated sources. In addition to the DC component, the light intensity attenuation, frequency domain systems can measure phase and modulated amplitudes which can all be related back to the input signal. Frequency domain method is mathematically related to TRS via Fourier transform. However, frequency domain systems have an advantage of being an inexpensive alternative to TRS systems. Also, in practice, frequency domain instruments display higher signal to noise ratio (SNR) and are generally faster than TRS instruments. The disadvantage of frequency domain systems is that they can only provide information at a finite number of modulation frequencies. An example of commercially available frequency domain system (ISS 96208) is shown in Figure 3.



*Figure 3.*    An example of frequency domain instrument. ISS, Inc.'s oximeter model 96208.

## 3.     Hemodynamic Response

### 3.1     Modified Beer-Lambert Law

By far, the most widely used model in calculating hemodynamic response is based on the classic Beer-Lambert law. The Beer-Lambert law is derived from solution to radiation transport equation under several simplifying assumptions [91]. It describes a linear relationship between absorbance, $A$, of light through a medium and wavelength dependent extinction coefficient, $\epsilon(\lambda)$. This relationship is given by **Equation (1)**

below.

$$A = -\log \frac{I}{I_0} = \epsilon(\lambda)cL \tag{1}$$

where $I = I_0 \exp -\epsilon(\lambda)cL$ is the intensity of the transmitted light, $I_0$ is the intensity of the incident light, $c$ is the concentration of the chromophore and $L$ is the path length. In continuous wave NIR imaging, a modification of the Beer-Lambert law has been successfully applied, albeit with some caveats due to inaccurate but simplifying assumptions about the biological media. Delpy et. al. were the first to introduce the modified Beer-Lambert law in [19, 17, 87]. Modified Beer-Lamber law (hitherto referred to as MBLL) relies on several simplifying assumptions. These were identified by Obrig and Villringer and are paraphrased below [78].

1 *High, but constant scattering in the media.*

2 *Homogeneous medium.*

3 *Homogeneous change of parameters of interest within each volume sampled.*

For non-scattering media, following the classical Beer-Lambert law, $L$ is equal to the distance between source and detector, denoted as $d$. For scattering media **Equation (1)** can be rewritten as

$$A = \epsilon(\lambda)c \cdot d \cdot DPF(\lambda) + G(\lambda) \tag{2}$$
$$= \epsilon(\lambda)c \cdot \langle L \rangle + G(\lambda) \tag{3}$$

where $G$ is the contribution of the attenuated light due to scattering and $DPF = \langle L \rangle / d$ is called the differential path length factor. The $\langle L \rangle$ is the mean path length of the detected photons [91]. The differential path length factor describes the increase in path length due to tissue scattering. The $DPF$ for various tissue samples have been both experimentally [21, 58] and numerically studied [41] and can easily be looked up on a table (for example, see [24]). Since the value of wavelength dependent $G$ is not generally known, it is not possible to assess the absolute value of $A$. Under the first assumption given above, $DPF$ and $G$ can be assumed to be constant. This allows for assessment of *changes* in chromophore concentration by subtracting out $G$. This is generally considered a plausible assumption when measuring hemodynamics since changes in oxygenation and concentration of hemoglobin affects the absorption coefficient more significantly than the scattering coefficient [78]. The **Equation (2)** can then be rewritten as

$$\Delta A = A_t - A_{t_0} = \epsilon(\lambda) \cdot \Delta c \cdot d \cdot DPF(\lambda) \tag{4}$$
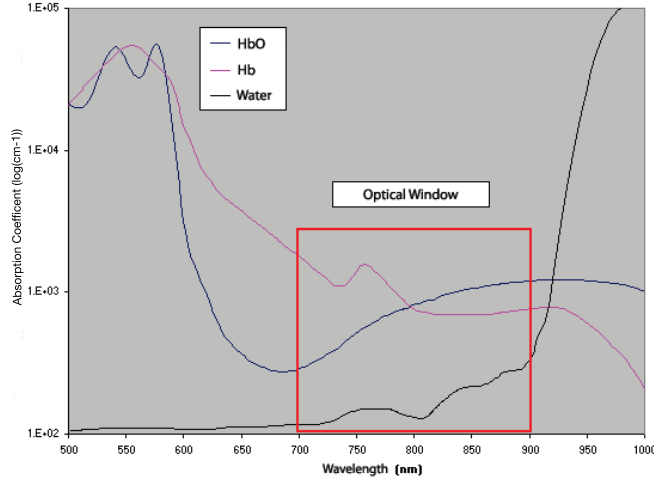
*Figure 4.* Graph of absorption coefficient versus wavelength of light. The optical window is denoted by the red box.

where $A_t$ is the absorbance at some time $t$ after the change in concentration of chromophores and $A_{t_0}$ is the initial absorbance.

Each chromophores have a distinguishable extinction spectrum in the visible to the near-infrared range. This allows for the measurement of concentration changes in several chromophores simultaneously by taking optical measurements at multiple wavelengths. The main chromophores in the optical window[1] of 600 to 900 nm, are oxy- and deoxy-hemoglobin (denoted HbO and Hb respectively), water, lipids and cytochrome-c-oxidase. Figure 4 shows the graph of the absorption coefficients of HbO, HbO and water versus wavelength. The NIR range is denoted by the rectangular window. The main chromophores of interest in nearly all studies of NIR spectroscopy based brain imaging are HbO and Hb, as the other chromophores' changes are orders of magnitude smaller than that of HbO and Hb [9, 79]. It should be noted that there have been studies where transient increase in cytochrome-oxidase redox was observed for visual stimulations [39, 57, 77]. However, there are some questions as to the detectability of changes in cytochrome-oxidase redox. Uludag et. al. report that concurrent detection of change in cytochrom-oxidase redox state with those of hemoglobin concentration and oxidation might suffer from severe cross-talk error where the magnitude of the error for the redox state of cytochrome-c-oxidase may be in the order of those detected experimentally [107]. Cross-talk error is a general problem for MMBL based NIR imaging and will be revisited in some detail later in the chapter.

Oxy- and deoxy-hemoglobins are mainly of interest because they are related to the regional cerebral blood flow (rCBF). The focal change in rCBF determines the *activation* state. The term activation usually refers to the focal increase in rCBF whereas a decrease is called deactivation [78]. With the dual wavelength approach, one can derive two simultaneous equations to be solved for each of the two chromophore concentration changes. To this end, **Equation (4)** is split into two parts, separating the contributions from HbO and Hb. **Equation (4)** is then, rewritten as

$$\Delta A(\lambda) = (\epsilon_{HbO}(\lambda)\Delta[HbO] + \epsilon_{Hb}(\lambda)\Delta[Hb]) \cdot DPF(\lambda) \cdot d \qquad (5)$$

where $\Delta[HbO]$ is the change in HbO concentration and $\Delta[Hb]$ is the change in Hb concentration. Given **Equation (5)**, and assuming $\epsilon(\lambda)$ can easily be looked up from the extinction spectra for each chromophores, concentration changes ascertained by solving the two simultaneous equations at two distinct wavelengths. The generalization to more than two wavelength is straight forward and can be found in [16].
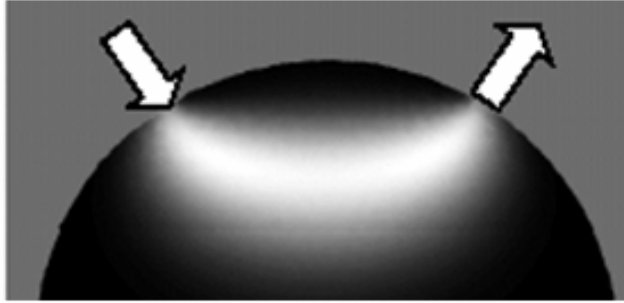
## 3.2    Some Issues Regarding MBLL



*Figure 5.*    The assumed banana-shaped light path through tissue sample

The simplifying assumptions of homogeneous medium and homogeneous change in differential volume are clearly inadequate for most biological media. The usual banana-shaped sampling volume [10, 108] from source to detector, as depicted in figure 5, is inadequate as the path of light is greatly affected by cerebrospinal fluid (CBF) [83] and the pial cerebral vessels on the surface of the brain [25]. This gives rise to a layered effect on the path of light that is not accounted for under the MBLL assumptions. The greater part of the problem lies in what is termed *partial volume effect*. Under the homogeneous change assump-

tion of MBLL, magnitude of concentration changes of chromophores are underestimated because the activated volume is usually smaller than the sampling volume [107]. Furthermore, the wavelength dependence of optical tissue properties means that this partial volume effect is wavelength dependent. As a result of this wavelength dependence, change in one chromophore concentration may mimic the effect of another, giving rise to crosstalk errors [84]. This is due to the fact that in the MBLL model, wavelength depedence is ignored by using a constant mean path length independent of wavelength. More precisely, focal hemodynamic change depends on the knowledge of the partial pathlength within the partial volume, which is unknown. Calculating the concentration changes of chromophores using measured absorbance changes at different wavelengths will give rise to distortions in the extinction spectra. There has been some progress in layered modeling based on Monte Carlo methods [96, 41]. Using Monte Carlo simulation, path length is estimated at each layer, which can be used to minimize the distortion and crosstalk.

There is some debate, as Obrig and Villringer point out [78], as to the significance of the crosstalk distortion. According to Obrig et. al.'s study, crosstalk between Hb and HbO elicits about 10% error. This is small enough that, although there is noticeable distortion on the ratio of magnitudes between chromophores, this will not significantly alter the quality of images.

**Diffuse Optical Tomography.** Boas et. al. in [9] suggested using a more sophisticated and accurate model for photon propagation in the brain to minimize the effect of crosstalk. In lieu of MBLL based image construction, Boas et. al. suggested a diffuse optical tomographic (DOT) method. The mathematical details of DOT methods are covered in [3, 4]. An excellent general review of DOT is given in [7]. Here, we limit ourselves to a very cursory overview of DOT method. The DOT is based on photon diffusion equation with Robin boundary conditions derived from radiation transport equation with less restrictive assumptions describing the propagation of light photons through a turbid medium. The diffusion equation is

$$-D(r)\nabla^2\Phi(\mathbf{r},t) + v\mu_a\Phi(\mathbf{r},t) + \frac{\partial\Phi(\mathbf{r},t)}{\partial t} = vS(\mathbf{r},t) \qquad (6)$$

where $\Phi(\mathbf{r},t)$ is the photon fluence at position $\mathbf{r}$ and time $t$, $S(\mathbf{r},t)$ is the source, $D = v/(3\mu_s')$ is the diffusion coefficient, $\mu_s'$ is the reduced scattering coefficient, $\mu_a = \epsilon(\lambda) \cdot c$ is the absorption coefficient and $v$ is the speed of light through the medium. Assumption under which **Equation (6)** accurately models photon propagation is that of scatter

dominated medium (same as the first assumption for MBLL model). The goal in DOT is to reconstruct the 3-D distribution of absorption and scattering coefficients of the medium given boundary data.

Under the first order Born approximation, the solution to **Equation (6)** is

$$\Phi_{sc}(\mathbf{r}_d) = - \int \Phi_{inc}(\mathbf{r}) \frac{v}{D} (\epsilon_{HbO}(\lambda)\Delta[HbO] + \epsilon_{Hb}(\lambda)\Delta[Hb]) G(\mathbf{r}, \mathbf{r}_d) d\mathbf{r}$$

(7)

where $G(\mathbf{r}, \mathbf{r}_d)$ is the Green's function, $\mathbf{r}_d$ is the location of the detector, $\Phi_{inc}$ stands for the incident photon fluence and $\Phi_{sc}(\mathbf{r}_d)$ denotes photon fluence at the detector. **Equation (7)** can be discretized by taking multiple measurements of $\Phi_{sc}(\mathbf{r}_d)$ at different source-detector positions. The integrand of **Equation (7)** describes the sensitivity of each measurement to the change in absorbance within each volume sample. For focal change in absorbance,

$$\Delta A = - \log \left( \frac{\Phi_{inc}(\mathbf{r}_s, \mathbf{r}_d) + \Phi_{sc}(\mathbf{r}_s, \mathbf{r}_d)}{\Phi_{inc}(\mathbf{r}_s, \mathbf{r}_d)} \right)$$

(8)

$$\approx \frac{\Phi_{inc}(\mathbf{r}_s, \mathbf{r}) G(\mathbf{r}, \mathbf{r}_d)}{\Phi_{inc}(\mathbf{r}_s, \mathbf{r}_d)} \frac{v d\mathbf{r}}{D} \Delta\mu_a$$

(9)

where $d\mathbf{r}$ is the differential volume over which the absorbance change occurs.

In general Rytov approximation provides better reconstruction than Born approximation [8]. Here, MBLL is approximated locally at each sampling volume and the effective path length is estimated using the Rytov approximation as

$$L_j = \Phi_{inc}(\mathbf{r}_s, \mathbf{r}_j)\Phi_{inc}(\mathbf{r}_j, \mathbf{r}_d)$$

(10)

Change in the absorption coefficient is found by arranging the measurements and voxel combinations in vector-matrix form as $y = Ax$ where $y$ is the change in absorbance detected at each source-detector pair, $A$ is the so called system matrix derived from $L_j$ and $x$ is the optical parameters of interest, namely the absorption coefficients.

## 3.3    Physiological Interpretations

The oxygenation response over an activated area of the cortex can be described by a *decrease* in Hb along with a simultaneous *increase* in HbO [78]. The accompanying increase in HbO is usually two to three times that of the decrease in Hb, hence the total volume of hemoglobin is expected to increase locally in the activated areas. Inversely, deactivation is typically characterized by decrease in HbO along with increase in

Hb. If both HbO and Hb increases or decreases, this may indicate origin other than cortical activity. Therefore, it seems prudent to report both Hb and HbO responses along with the total hemoglobin displacement. Recording Hb response has an added benefit that it can be related to and compared with fMRI blood oxygenation level dependent (BOLD) response as increase in the BOLD contrast is highly correlated with a decrease in Hb.

**Comparison with fMRI BOLD Response.**    A number of studies, comparing fMRI data with those gathered through NIR spectroscopy have been conducted [56, 72, 32, 105, 99, 106]. Such studies have addressed the problems of localization of detected signal and sensitivity of optical measurements to brain tissue [99]. Most of these studies have shown a high temporal negative correlation between BOLD and Hb responses [32] that confirms theoretical ideas about the nature of the BOLD response. The studies also show a good spatial collocation between BOLD and hemodynamic responses [56, 105]. Strangman et. al.'s study is of some interest since their results deviate from the expected results [99]. They observed that correlation between BOLD and Hb responses were highly variable between subjects. They've argued that this variability was due to the model error arising from simplifying assumptions described in the previous section. To account for these potential sources of errors, Strangman et. al. normalized each hemodynamic response for each subject separately with normalization factor equal to the ratio of the vascular response of interest and inverse BOLD response. Even so, their study found that correlation between BOLD and HbO were higher than between BOLD and Hb. This may be due to higher sensitivity of the optical measurement to changes in HbO.

**Sources of Physiological Noise.**    Despite the apparent importance of Hb, in the literature, the change in HbO is most widely reported and sometimes is the sole response reported. HbO is sometimes preferred due to its higher sensitivity to NIR based measurements than Hb. However, HbO measurements are not without disadvantages. There have been some studies (see for example [77, 22, 23, 47]) which indicate the presence of low frequency modulation ($\sim 0.1$ Hz) of both vascular (Hb, HbO) and metabolic (cytocrhome-c-oxidase) responses to visual stimuli with unknown origin. The cause of these low frequency oscillations are not exactly known but are usually attributed to extracerebral activities such as respiration. Obrig et. al. have found that these modulations are most significantly expressed in the HbO responses and thus is most susceptible to extracerebral noise [77]. These low frequency oscillations

12

are known collectively as Mayer wave and should be accounted for when analyzing data. Other sources of physiological noise are oscillations due to heartbeat and signal displacement due to motion artifacts. The oscillations due to heartbeat is faster than Mayer wave ($\sim 1$ Hz) [98, 44].

**Removing Physiological Noise.** One method of removing the low frequency artifact is to convolve the response signal with a model of stimulus signal. Such methods have been used to increase the SNR in fMRI [54]. The stimulus signal is usually modeled as a pulse train with evenly spaced interstimulus interval as in **Equation (11)**

$$s(t) = \sum_{m=1}^{M} \delta(t - m\tau_{ISI}). \tag{11}$$

Here, $M$ is the total number of stimulis and $\tau_{ISI}$ is the interstimulus interval. The convolved signal is used to fit a generalized regression model of the form

$$x(t) = \sum_{b=1}^{N} g_b(t \mod \tau_{ISI})\beta_b + e(t) \tag{12}$$

where the response signal $h(t) = \sum_{b=1}^{N} g_b(t)\beta_b$, is expressed as a linear combination of basis functions $g_b(t)$. **Equation (12)** can be rewritten in matrix form and generalized linear regression method can be used to fit $\beta_b$ (see [59] for a review of linear regression).

Gratton et. al. in [34] describes a least squares regression method to model heartbeat artifacts and to filter it out adaptively. Since the heartbeat rate is approximately 1 Hz, it is necessary that data is sampled at a sufficiently high rate (e.g. above the Nyquist rate) so as to represent and filter the artifacts out correctly and have minimal impact on the signal of interest itself [98].

Izzetoglu et. al. have suggested an adaptive filtering technique for motion artifact cancellation using complementary sensors to sense motion [49]. Wiener filtering was proposed as a sensor-free alternative to adaptive filtering in [20]. Wiener filtering is a well established least squares method of reconstructing a signal degraded by motion artifacts. It is widely used in image processing and other signal processing fields. Suppose the response signal is modelled as the true signal contaminated by additive stationary noise (the motion artifact), i.e. by $h(t) = x(t) + w(t)$. The idea is to construct a filter $g(t)$ or $G(\omega)$ in the frequency domain such that mean square error is minimized between the real signal $x(t)$ and the estimated signal $\hat{x}(t) = g(t) * y(t)$ where $*$ denotes the convolution operator. Without going into the details of the derivation, it turns

out that the optimal filter $G(\omega)$ in the Fourier domain is

$$G(\omega) = \frac{P_x(\omega)}{P_x(\omega) + P_w(\omega)} \tag{13}$$

where $P_x(\omega)$ and $P_w(\omega)$ are the power spectral density functions of the signal and noise, repsectively. One disadvantage with this method of motion artifact removal is the estimation of $P_x$ and $P_w$, which are not known a priori.

Zhang et. al. describes a new method based on eigenvalue decomposition [116]. This method differs fundamentally from others in that it uses spatial filtering instead of temporal filtering that previous methods employ. The justification for this line of thinking is that the physiological noise is usually systematic and global, whereas stimulus driven activation resides locally. The approach uses principle component analysis (PCA) to extract a set of basis functions, orthogonalize them, and use them to filter the signal. Let $\mathbf{H}_s$ and $\mathbf{H}_b$ denote the values of changes in hemodynamic response during the stimulation and rest (baseline) periods respectively, where each column corresponds to a channel or spatial location and each row corresponds to a time instance. Then, the matrix to be decomposed is the spatial correlation matrix

$$\mathbf{C} = (1/N)\mathbf{H}_b\mathbf{H}_b^T \tag{14}$$

where $N$ is the total number of time samples. Then, the first $M$ number of eigenvectors are chosen as the basis, $\mathbf{U}_{base} = [\mathbf{u}_1 \ldots \mathbf{u}_M]$. The filtered stimulus invoked signal is then

$$\tilde{\mathbf{H}}_{\mathbf{s}} = (\mathbf{I} - \mathbf{U}_{base}\mathbf{U}_{base}^T)\mathbf{H}_s. \tag{15}$$

## 4.     Neuronal Response

The acquisition of neuronal response using noninvasive NIR spectroscopy is less well-known than the slower hemodynamic response. However, there is a great deal of potential for its development and verification via comparison with other modalities such as event-related potentials (ERP) [32]. The origins of optically sensing this fast signal (usually known as intrinsic optical signal or IOS for short) can be traced back to Cohen [14]. Cohen showed that neuronal activity elicits a fast change in light scattering of neural tissue. These properties were confirmed in invasive experiments where an isolated nerve and tissue slices electrically stimulated and optical properties measured simultaneously [14, 103, 104, 90]. Similar agreement between electrophysiological signal and light scattering change following stimulation is reported in [97].

Fast scattering changes were also observed on macroscopic structures. Frostig et. al. observed the IOS changes in hippocampal slices [29]. Experiments on exposed cortex of animals also confirmed the presence of scattering changes [66, 86].

Initial studies in detecting these scattering changes involved visual stimuli [33, 68] and tapping task [37] and used frequency domain methods [35]. Such a method is termed event-related optical signal (EROS). In EROS, frequency domain instrument is used at millisecond temporal resolution to detect phase shift of the photon density at the detectors [38]. With the phase information, it is possible to gauge the average time of flight of photons detected and thus infer the average path length. With this path length information, it is, in principle, possible to better localize the signal (compare to MBLL approach using CW equipment) by estimating roughly the depth that the photons travel [36]. Measuring phase information for detection of IOS seems, at first, principled since it has been shown that phase measurements are more sensitive to scattering changes than to absorption [30]. However, other studies have reported that the intensity data yield higher SNR [95, 26, 112]. Recently, Maclin et. al. examined fast signal response in somatosensory cortex to electrical stimulation of the median nerve recording both phase and intensity data simultaneously [62].

## 4.1    Data Analysis

Franceschini et. al. has employed a simple back-projection method described in [28] to create an optical image of the probed region. In this method the region of interest is discretized and each pixel is assigned a set of source contribution with weights. Each pixel is then a weighted combination of the signal from different sources. In this method, intensity signal is also first converted to a change in absorption coefficient using differential pathlength factor (DPF) approach described by Cope and Delpy in [17]. With EROS approach, the usual method of data analysis is to cross-correlate the signal, either phase or amplitude or both, with the stimulus signal. Also, in order to reduce erroneous reading due to equipment sensitivity to changes in superficial regions under source or detector fiber, cross-correlation between individual channels are assessed [32].

Removing physiological artifacts from fast signal is similar to removing artifacts from slow signal. For removing heartbeat artifact, the same approach described previously is used where a least-squares fit model of each pulse is constructed then subtracted out. For Mayer wave, since the fast signal dynamics is orders of magnitude faster than the oscillations

of Mayer wave, it is possible to filter out the drift by simply employing a high-pass filter.

## 5.     Human Subject Studies

Since the early 90s, noninvasive functional brain imaging of humans using NIR methods have been slowly gaining momentum despite existence of more established imaging modailties, such as PET, fMRI, and EEG. Part of the reason as stated previously, is because of its relatively high temporal resolution and its ability to monitor multiple tissue chromophores. The technique has been applied to adult as well as infant studies. NIR method is particularly suited for infant studies as the equipment, at least the CW kind, are minimally restraining, relatively safe, and portable [67]. Most neonatal studies focus on sensory stimulation such as visual, auditory and olfactory stimulations [69, 101, 89, 115, 6, 5], and cerebral disfunction [70, 71]. Our review will focus primarily on adult studies with some emphasis on defense and security applications.

Adult subject studies can be divided into two broad categories; response to basic sensory stimulation and response to more complex cognitive tasks. Recently, there have also been reports applying the NIR spectroscopy to brain computer interface research [18] and studyinh the correlation of hemodynamic response to computational cognitive models [94].

**Motor and Sensorimotor Stimulation Studies.**     Maki et. al. has conducted studies on hemodynamic response to opposing finger movement stimuli in [64, 65]. They observed a significant increase in HbO and total blood volume and decrease in Hb as expected for cortical activation. Watanabe et. al. and Hirth et. al. conducted similar studies corroborating the results of Maki et. al. [111, 42]. Kleinschmidt et. al. also performed finger opposition task using NIR spectroscopy simultaneously with fMRI [56]. Colier et. al. studied response to coordinated movements of hands and feet both in phase and in anti-phase. Expected activation pattern was observed with decrease in Hb and increase in HbO with more significant changes seen in HbO. They found no significant difference between in phase and anti-phase stimulations [15]. Miyai et. al. conducted a more sophisticated study observing sensorimotor cortical response to human gait. This study is noteworthy, in that, due to its constraining nature, it is not possible to study such a paradigm with fMRI. The subjects were measured during a 30 second treadmill walking. They report observing an increase in the level of HbO and total blood volume after 3 to 5 seconds while seeing slight decrease in Hb level [74].

Bilateral study was conducted by Franceschini et. al. using multiple stimulus. The volunteers were subjected to opposing finger, finger tapping, and medial nerve stimulations. They saw a consistent increase in HbO and decrease in Hb in the cortical region contralateral to the side stimulated [27].

**Visual Stimulation Studies.** Visual stimulations have also been studied in adult human subjects. Meek et. al. stimulated their subject by subjecting the volunteers to a 30s on/off cycles of computer graphics display [68]. They observed an increase in HbO and total blood volume during stimulation in the occipital cortex. They compared this with a measurement on frontal lobe which resulted in no significant change confirming the role of occipital cortex during visual stimulation. Heekeren et. al. conducted similar study with sustained two minute stimulation [40]. They observed an increase in HbO during the first 19 seconds of stimulation then plateauing during the entirety of the stimulation. The time-course of Hb was more dynamic. An initial decrease during the first 13 seconds was observed after which the subsequent 10 seconds saw an increase plateauing to a new level, near the baseline, after 40 seconds or so. After the stimulation was shut off Hb started to increase beyond the baseline.

**Language Studies.** Watanabe et. al. conducted language dominance study on 11 healthy subjects and 6 subjects with intractable epilepsy [110]. A word generation task was conducted, each lasting 17 seconds with 60 second rest period. The group saw increase in HbO, total blood volume, and Hb which seceded after the end of stimulation period for both types of subjects. This result is distinctly different from normal patterns of activation. The study unfortunately did not address this point. They corroborated their results of dominant hemisphere with Edinburgh questionnaire for health subjects and Wade test for epileptic subjects. Sakai et. al. examined speech processing using NIR spectroscopy [92, 88]. In their study, they used auditory stimulation where subjects were asked to track targets and press a button when the target shifted from one ear to another. They conducted two tasks; a repeat task where target was the repetition of a single sentence within a task block; and a story task where a target was a different successive sentences of one continuous story. They found, consistent with fMRI results, that compared to the repeat task, story task was localized to the left superior temporal cortex. Also, story task saw a larger increase in HbO and decrease in Hb compared to white noise control task. Language lateralization was also studied by Kennan et. al. [55] and Noguchi et. al.

[75]. Kennan's group used visual stimulation where subjects were asked to find syntactic and semantic errors in sentences presented. All subjects showed left hemispherical dominance to varying degree. The NIR spectroscopy results were compared with results garnered from fMRI modality where good consistency was found between the two. Similar error detection task but, using auditory stimuli instead, was conducted by Noguchi et. al. The error detection task was split into two, syntactic and semantic. Compared to the syntactic task, semantic task show very little activation in the left hemisphere. In the right hemisphere both task showed little activation, suggesting as with Kennan's group, that language processing is dominant in the left hemisphere.

**Mental Health Studies.**     Number of studies have been produced concerning subjects with brain disfunction, such as epilepsy [1], depression [100], and Alzheimers [43]. Adelson et. al. reports on the use of NIR spectroscopy on epileptic patients. They saw a preictal increase in oxygenation level 1 and 2 hours before and a decrease in oxygenation during seizure period [1]. A verbal fluency task was given to Alzheimer's patients and normal subjects by Hock et. al. They observed a decrease in HbO during the task in Alzheimer's patient in contrast to increase in HbO in normal subjects. Both groups saw slight decrease in Hb [43]. Suto et. al. conducted verbal fluency and finger tapping tasks on patients with depression, patients with schizophrenia and normal subjects. Compared with the normal subjects (control), depression patients saw smaller HbO increase during the first half of the verbal fluency task period whereas, schizophrenic patients were characterized by a small dip in the HbO during the start of the task and a re-increase in the post task period. The HbO increase in depression patients were generally larger than those of the control group. No significant difference was found between control and schizophrenic patients [100].

**Cognitive Tests.**     Schroeter et. al. studied hemodynamic responses to classic Stroop task where mismatch in words spelling out various colors [93]. The task consisted of two rows and were asked to decide whether the color of the top row of letter corresponded with the bottom row spelling out a color. Three types of stimuli were presented, (1) neutral, where top row consisted of X's, (2) congruent, where top row was a word spelling out some color and bottom row matched the color of the top row, and (3) incongruent where the bottom row mismatched with the color on the top row. Incongruent stimulus generated the largest rise in HbO and and largest decrease in Hb, congruent being second

largest and neutral being the least activated. This result agrees with the intuition that the most difficult task would see the most activation.

Izzetoglu et. al. used target categorization and N-back tasks to assess hemodynamic responses in [50, 51]. In the oddball target categorization task the subject was given two stimuli, one more frequently occurring than the other. The objective was to press a button when the less frequent stimulus was given. They found that oxygenation change was higher when presented with less frequent stimulus. In the N-back task, 2-back saw the largest average oxygenation change with consistent rise from 0-back. However, 3-back had lower average oxygenation than 2-back. The group explained this result as a consequence of the difficulty exceeding the subject's ability to keep up with their working memory.

Recently, NIR spectroscopy also found application in analyzing more complex cognitive tasks and in workload assessment. These studies are of interest to defense and security researchers as they attempt to assess the cognitive state of the subject while the subject is given a series of tasks involving a cognitive function, such as problem solving or memory recall. Izzetoglu, et. al. for instance, studied oxygenation response to guilty knowledge task (GKT) which is commonly used to model deception [51]. An fMRI study using similar task setup was performed by Langelben et. al. [60]. These studies point to potential use of NIR based noninvasive brain monitoring as a lie detector. Both studies involved display of playing cards that are divided into four different categories, lie card, truth card, control card, and non-target cards. One card was shown for 3 seconds with 12 second interstimulus interval between each card. For truth, lie, and non-target cards, the subjects were asked, "do you have this card?" For the control cards, the subjects were asked, "is this the [control card]?" The subject was asked to lie about the lie card only. The goal was to see if the level of hemodynamic response differed significantly between lie and truth responses. Izzetoglu et. al. found that in 8 out of the 13 subjects, the level of the oxygenation change during the lie was higher than the level during the truth. Figure 6 shows the average oxygenation response of two subjects, averaged over all sixteen channels in the system used by Izzetolgu et. al. as reported in [51]. Correspondingly, Langelben's study found that lies elicited a rise in BOLD response in several areas including the anterior cingulate cortex, the superior frontal gyrus, and left premotor, motor, and anterior parietal cortex. The results of the two studies cannot be compared straightforwardly as Izzetoglu's system covered only the frontal lobe area and their results saw significant difference in almost all channels except one (see table 1). In contrast, the BOLD response were localized in
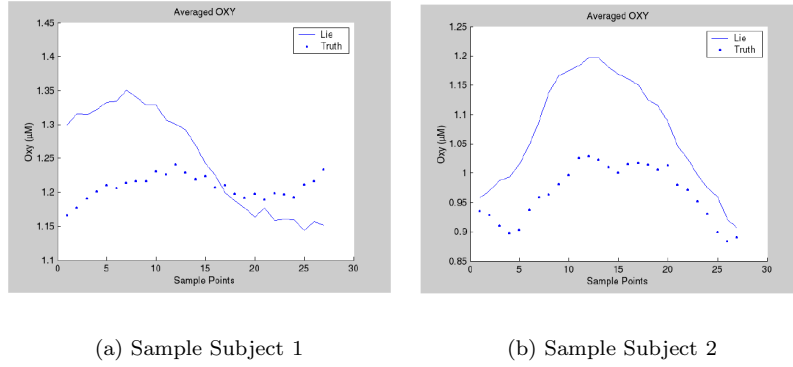
(a) Sample Subject 1        (b) Sample Subject 2

*Figure 6.*    Averaged oxygenation response for two subjects for GKT, ©2002 IEEE

| Ch1: | Ch3: | Ch5: | Ch7: | Ch9: | Ch11: | Ch13: | Ch15: |
|------|------|------|------|------|-------|-------|-------|
| 96.96% | 88.14% | 100% | 100% | 99.97% | 100% | 100% | 100% |
| Ch2: | Ch4: | Ch6: | Ch8: | Ch10: | Ch12: | Ch14: | Ch16: |
| 100% | 100% | 100% | 100% | 100% | 100% | 21.6% | 100% |

*Table 1.*    t-test results for GKT with $\alpha = 0.05$, the numbers shown are the results of $1 - P$ where $P$ is the probability calculated at the given $\alpha$. ©2002 IEEE

several areas with perhaps the superior frontal gyrus as the region most likely corresponding to Izzetoglu's results.

Several of studies using NIR technolgy examined the potential for military applications by monitoring subject's hemodynamic response to simulations of complex military-related tasks with variable levels of difficulty. Takeuchi examined hemodynamic response to flight simulation tasks [102]. In it, an aircraft landing procedure was simulated. The aircraft was modeled after Japanese Air Self Defense Force (JASDF) T-2 jet trainer. The procedure for the task consisted of a minute of rest with eyes closed, then one minute of simulated level flight after which the subjects were instructed to descend under variable wind conditions. After the touchdown, the subjects were instructed to taxi the simulated aircraft along the runway center line and then brake to a full-stop as quickly as possible. Rise in HbO level in the left forehead was observed during the descent phase with peaks during the touchdown or the taxi phase (see figure 7). Takeuchi reports that the amount of increase in HbO varied directly with increase in wind velocity simulated. He also reports seeing little to no change in Hb level (see figure 8).

Izzetoglu et. al. conducted a study where air warfare management was simulated using Warship Commander (WC) task developed by Pacific
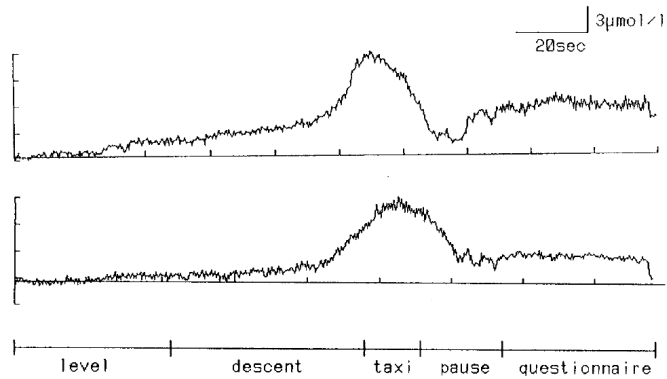
*Figure 7.* Change in HbO on the left forehead under 20 knot crosswind. Maximum amplitude is observed either during the touchdown (upper) or during the taxi phase (lower). ©2000 J. Occup. Health
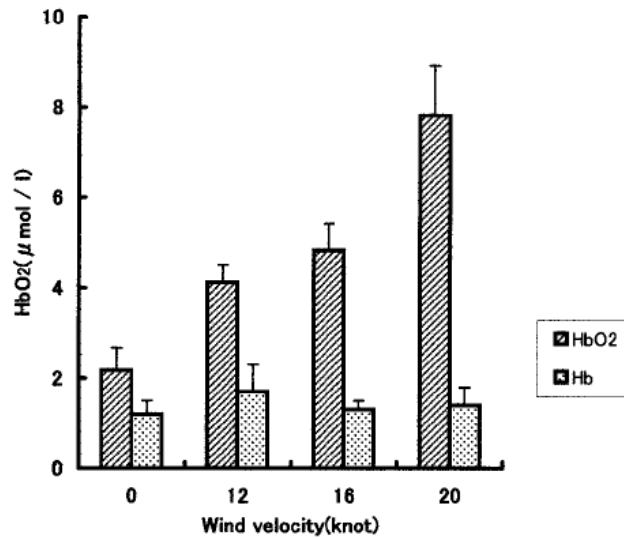


*Figure 8.* Averaged HbO and Hb on the left forehead under different wind conditions ©2000 J. Occup. Health

*Figure 9.* Warship Commander Simulator. The yellow colored tracks represent a more difficult track.

Science and Engineering Group under the guidance of Space and Naval Warfare Systems Center. Figure 9 shows a screen capture of the simulator. The objective of the task is to identify different aircrafts or tracks that appear on the screen as "friendly" or "hostile" and act accordingly while simultaneously monitoring ship status and communication. The difficulty was varied by varying the number of aircrafts and number of more difficult "yellow" tracks. They found that as number of aircrafts per wave increased, an increase in oxygenation level was observed with the lowest setting (6 aircrafts per wave) eliciting oxygenation decrease (see figure 10).

Our own work attempted to correlate the hemodynamic response to an auditory task with simulated response using ACT-R computational cognitive model. For reference on ACT-R model, see [2]. The subjects were given audio stimuli at varying interstimulus intervals (6, 4, 2, and 1 seconds). The task was divided into four 10 minute blocks with each block further divided into eight 72 second intervals, during which interstimulus interval remained constant, with at least 10 second rest period between each interval and a 2 minute rest between blocks. Our goal was to correctly identify the workload, as defined by the interstimulus intervals, from the hemodynamic responses. There were eight examples of
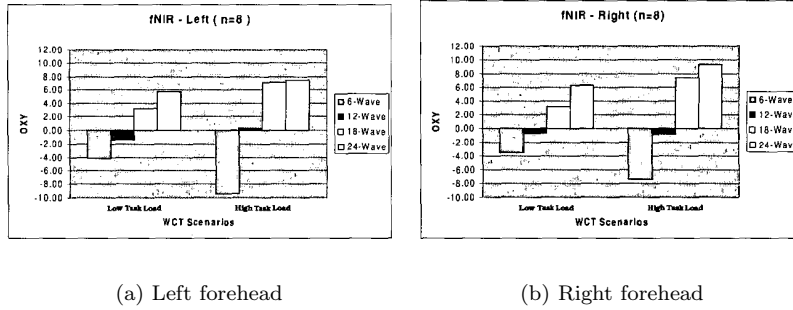
(a) Left forehead               (b) Right forehead

*Figure 10.*    Averaged oxygenation level for left and right forehead for varied number of aircrafts for high and low task load corresponding to the number of "yellow" tracks.
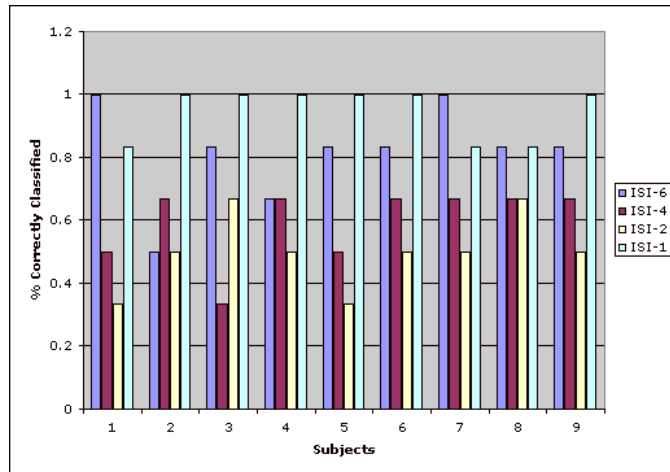


*Figure 11.*    Percentage of correct classification for each workload for 9 subjects.

each interstimulus intervals. We trained using two examples of each interstimulus interval. The result of the classification is given in figure 11. The best result were obtained for the highest workload (interstimulus interval of 1 second) with the most confusion found in the middle two. These results, we found, were in agreement with ACT-R simulation in that ACT-R found the 1 second interval to be an "overloaded" condition and predicted that the response time needed was a little over 1 second. Thus, the response for 1 second interstimulus interval was expected to be more highly differentiable from the rest.

## 6.     Concluding Remarks and Future Directions

To summarize, current state of NIR research consists of two major groups of instrumentation; (1) continuous wave and (2) time-resolved and frequency domain; and two major groups of parameters assessed (1) slow responding hemodynamic (HbO and Hb) parameters and (2) fast response neuronal parameter. Assessing the fast response parameter requires high temporal resolution provided by NIR equipment. Such temporal resolutions are currently not possible using fMRI modality. Thus, a natural complementary relationship exists between fMRI and NIR methods, where fMRI can provide better spatial localization and NIR better temporal resolution.

A preference of hemodynamic response is mainly due to better contrast-to-noise ratio and the ease of comparability with fMRI BOLD response which is inversely related to changes in Hb, over measurement of neuronal activity. However, measurement of the fast neuronal response can potentially benefit NIR methods by addressing the inherent pitfalls of MBLL assumptions in slow response measurements. Fast response, aside from being a direct measurement of neuronal activity, also has the potential to provide better spatial resolution.

Another promising alternative to the rather restrictive MBLL model is the layer model using diffusion equation. Diffuse optical imaging provides a better model for photon migration where approximation of path length is possible. This would provide a much improved focal change information and potentially eliminate crosstalk noise.

The major difficulty in any functional brain studies is inter-subject comparisons. Essentially, all NIR functional brain studies report high variability between subjects. No true comparison can be made due to relative nature of hemodynamic data. Since path length is unknown under MBLL, it is not possible to assess absolute levels of hemodynamic parameters. Instead, each subject is compared with their own baseline measurements. However, generally speaking, the shape of the time evolution of the signals are similar between subjects and thus can be analyzed using qualitative comparisons.

There are several future directions that NIR brain sensing and imaging research can take. In instrumentation, advances in time-resolve spectroscopic equipment may yield less expensive equipment and thus a more prolific use. This will allow for approximation of time of flight parameter providing a possible avenue for inferring path length. Theoretically, there is a need for better theoretical modeling to eliminate crosstalk noise. Possible improvements have already been introduced by Boas, et. al [8]. However, more human subject studies need to be conducted to

verify the feasibility of the model. Also, diffuse optical imaging is computationally more intensive than the MBLL based methods. Task specific variations in source-detector arrangements may also provide higher resolution in the areas of interest. A more dense arrangement would naturally provide better spatial resolution although there is a physical limit as the signal must penetrate through the skull. The authors acknowledge that the field is still young and results are preliminary. As a consequence the field provides abundance of research opportunities.

## Notes

1. The term "optical window" denotes the spectral range where a low absorption by chromophores allow for significant penetration of light.

## References

[1] P. D. Adelson, E. Nemoto, M. Scheuer, M. Painter, J. Morgan, and H. Yonas. Noninvasive continuous monitoring of cerebral oxygenation periictally using near-infrared spectroscopy: a preliminary report. *Epilepsia*, 17:89–99, 2002.

[2] J. R Anderson and C. Lebiere. *The Atomic Components of Thought*. Lawrence Erlbaum Associates, 1998.

[3] S. R. Arridge. Photon measurement density functions. part 1: Analytical forms. *Applied Optics*, 34:7395–7409, 1995.

[4] S. R. Arridge. Optical tomography in medical imaging. *Inverse Problems*, 15:R41–R93, 1999.

[5] M. Bartocci, J. Winberg, G. Papendieck, T. Mustica, G. Serra, and H. Lagercrantz. Activation of olfactory cortex in newborn infants after odour stimulation. *Pediatric Research*, 50:324–330, 2001.

[6] M. Bartocci, J. Winberg, C. Ruggiero, L. Begqvist, G. Serra, and H. Lagercrantz. Activation of olfactory cortex in newborn infants after odour stimulation. *Pediatric Research*, 48:18–23, 2000.

[7] D. A. Boas, D. H. Brooks, E. L. Miller, C. A. DiMarzio, M. Kilmer, R. J. Gaudette, and Q. Zhang. Imaging the body with diffuse optical tomography. *IEEE Signal Processing Magazine*, 18(6):57–75, 2001.

[8] D. A. Boas, A. M. Dale, and M. A. Franceschini. Diffuse optical imaging of brain activation: approaches to optimizing image sensitivity, resolution, and accuracy. *NeuroImage*, 23:S275–S288, 2004.

[9] D. A. Boas, T. Gaudette, G. Strangman, X. Cheng, J. J. Marota, and J. B. Mandeville. The accuracy of near infrared spectroscopy and imaging during focal changes in cerebral hemodynamics. *NeuroImage*, 13:76–90, 2001.

[10] R. F. Bonner, R. Nossal, S. Havlin, and G. H. Weiss. Model for photon migration in turbid biological media. *Journal of the Optical Society of America A*, 4(3):423–432, 1987.

[11] B. Chance, E. Anday, S. Nioka, S. Zhou, L. Hong, K. Worden, C. Li, T. Murray, Y. Ovetsky, D. Pidikiti, and R. Thomas. A novel method for fast imaging of brain function, non-invasively, with light. *Optical Express*, 2(10):411–423, 1998.

[12] B. Chance, J. S. Leigh, H. Miyake, D. S. Smith, S. Nioka, R. Greenfield, M. Finander, K. Kaufman, W. Lery, M. Yong, P. Cohn, H. Yoshioka, and R. Boretsky. Comparison of time-resolved and unresolved measurement of deoxy hemoglobin in brain. In *Proceedings of National Academy of Science*, pages 4971–4975, 1988.

[13] B. Chance, S. Nioka, J. Kent, K. McCully, M. Fountain, R. Greenfeld, and G. Holtom. Time-resolved spectroscopy of hemoglobin and myoglobin in resting and ischemic muscle. *Anal. Biochem.*, 174:698–707, 1988.

[14] L. B. Cohen. Changes in neuron structure during action potential propagation and synaptic transmission. *Physiological Review*, 53:373–413, 1973.

[15] W. N. Colier, V. Quaresima, B. Oeseburg, and M. Ferrari. Human motor-cortex oxygenation changes induced by cyclic coupled movements of hand and foot. *Experimental Brain Research*, 129:457–461, 1999.

[16] M. Cope. *The development of a near-infrared spectroscopy system and its application for noninvasive monitoring of cerebral blood and tissue oxygenation in the newborn infant.* PhD thesis, University College London, London, 1991.

[17] M. Cope and D.T. Delpy. System for long-term measurement of cerebral blood flow and tissue oxygenation on newborn infants by infra-red transillumination. *Medical and Biological Engineering and Computing*, 28:289–294, 1988.

[18] S. Coyle, T. Ward, C. Markham, and G. McDarby. On the suitability of near-infrared (nir) systems for next-generation brain-computer interfaces. *Physiological Measurement*, 25:815–822, 2004.

[19] D. T. Delpy, M. Cope, P. van der Zee, S. Arridge, S. Wray, and J. Wyatt. Estimation of optical path length through tissue from direct time of flight measurements. *Physics in Medicine and Biology*, 33:1433–1442, 2004.

[20] A. Devaraj, M. Izzetoglu, K. Izzetoglu, S. C. Bunce, C. Y. Li, and B. Onaral. Motion artifact removal in FNIR spectroscopy for real-world applications. In *Nondestructive Sensing for Food Safety, Quality, and Natural Resources. Edited by Chen, Yud-Ren; Tu, Shu-I. Proceedings of the SPIE, Volume 5588, pp. 224-229 (2004).*, pages 224–229, October 2004.

[21] A. Duncan, J. H. Meek, M. Clemence, C. E. Elwell, L. Tyszczuk, M. Cope, and D. Delpy. Optical path length measurements on adult head, calf and forearm and the head of newborn infants using phase resolved spectroscopy. *Physics in Medicine and Biology*, 40:295–304, 1995.

[22] C. E. Elwell, H. Owen-Reece, J. S. Wyatt, M. Cope, E. O. Reynolds, and D. T. Delpy. Influence of respiration and changes in expiratory pressure on cerebral hemoglobin concentration measured by near infrared spectroscopy. *Journal of Cerebral Blood Flow and Metabolism*, 16:353–357, 1996.

[23] C. E. Elwell, R. Springett, E. Hillman, and D. T. Delpy. Oscillations in cerebral hemodynamics. implications for functional activation studies. *Advances in Experimental and Medical Biology*, 471:57–65, 1999.

[24] M. Essenpreis, C. E. Elwell, M. Cope, and D. T. Delpy. Spectral dependence of temporal point spread functions in human tissues. *Applied Optics*, 32:418–425, 1993.

[25] M. Firbank, E. Okada, and D. T. Delpy. A theoretical study of the signal contribution of regions of the adult head to near-infrared spectroscopy studies of visual evoked responses. *NeuroImage*, 8:69–78, 1998.

[26] M. A. Franceschini and D. A. Boas. Noninvasive measurement of neuronal activity with near-infrared optical imaging. *NeuroImage*, 21:372–386, 2004.

[27] M. A. Franceschini, S. Fantini, J. H. Thompson, J. P. Culver, and D. A. Boas. Hemodynamic evoked response of the sensorimotor cortex measured noninvasively with near-infrared optical imaging. *Psychophysiology*, 40:548–560, 2003.

[28] M. A. Franceschini, V. Toronov, M. E. Filiaci, E. Gratton, and S. Fantini. Online optical imaging of the human brain with 160-ms temporal resolution. *Optics Express*, 6(3):49–57, 2000.

[29] R. D. Frostig, E. E. Lieke, D. Y. Ts'o, and A. Grinvald. Cortical functional architecture and local coupling between neuronal activity and the microcirculation revealed by in vivo high-resolution optical imaging of intrinsic signals. *Proceedings of National Academy of Science USA*, 87:6082–6086, 1990.

[30] E. Gratton, S. Fantini, M. A. Franceschini, G. Gratton, and M. Fabiani. Measurements of scattering and absorption changes in muscle and brain. *Philosophical Transactions Royal Society of London*, 352:727–735, 1997.

[31] E. Gratton, W. W. Mantulin, M. J. vandeVen, J. B. Fishkin, M. B. Maris, and B. Chance. The possibility of a near-infrared optical imaging system using frequency-domain methods. In *Proceedings of of 3rd International Conference on Peace through Mind/Brain Science*, pages 183–189, 1990.

[32] E. Gratton, V. Toronov, U. Wolf, M. Wolf, and A. Webb. Measurement of brain activity by near-infrared light. *Journal of Biological Optics*, 10(1):011008–1–011008–13, 2005.

[33] G. Gratton, P. M. Corbaliis, E. Cho, M. Fabiani, and D. Hood. Shades of grey matter: non-invasive optical images of human brain responses during visual stimulation. *Psychophysiology*, 32:505–509, 1995.

[34] G. Gratton and P. M. Corballis. Removing the heart from the brain: Compensation for the pulsatile artifact in the photon migration signal. *Psychophysiology*, 32:292–299, 1995.

[35] G. Gratton and M. Fabiani. The event-related optical signal: a new tool for studying brain function. *International Journal of Psychophysiology*, 42:109–121, 2001.

[36] G. Gratton and M. Fabiani. Shedding light on brain function: the event-related optical signal. *Trends in Cognitive Sciences*, 5(8):357–363, 2001.

[37] G. Gratton, M. Fabiani, D. Friedman, M. A. Franceschini, S. Fantini, and E. Gratton. Photon migration correlates of rapid physiological changes in the brain during a tapping task. *Journal of Cognitive Neuroscience*, 7:446–456, 1995.

[38] G. Gratton, A. Sarno, E. Maclin, P. M. Corballis, and M. Fabiani. Toward noninvasive 3-d imaging of the time course of cortical activity: Investigation of the depth of the event-related optical signal. *NeuroImage*, 11:491–504, 2000.

[39] H. R. Heekeren, M. Kohl, H. Obrig, R. Wenzel, W. v. Pannwitz, S. Matcher, U. Dirnagl, C. E. Cooper, and A. Villranger. Noninvasive assessment of changes in cytochrom-c-oxidase oxidation in human subjects during visual stimulation. *Journal of Cerebral Blood Flow and Metabolism*, 19:592–603, 1999.

[40] H. R. Heekeren, H. Obrig, R. Wenzel, K. Eberle, J. Ruben, K. Villringer, R. Kurth, and A. Villringer. Cerebral haemoglobin oxygenation during sustained visual stimulation - a near-infrared spectroscopy study. *Philosophical Transactions: Biological Sciences*, 352:743–750, 1997.

[41] M. Hiraoka, M. Firbank, M. Essenpreis, M. Cope, S. R. Arridge, P. van der Zee, and D. T. Delpy. A monte carlo investigation of optical pathlength in inhomogeneous tissue and its application to near-infrared spectroscopy. *Physics in Medicine and Biology*, 38:1859–1876, 1993.

[42] C. Hirth, H. Obrig, K. Villringer, A. Thiel, J. Bernarding, W. Muhlnickel, H. Flor, U. Dirnagl, and A. Villringer. Non-invasive functional mapping of the human motor cortex using near-infrared spectroscopy. *NeuroReport*, 7:1977–1981, 1996.

[43] C. Hock, K. Villringer, F. Muller-Spahn, R. Wenzel, H. Heekeren, S. Schuh-Hofer, M. Hofmann, S. Minoshima, M. Schwaiger, U. Dirnagl, and A. Villringer. Decrease in parietal cerebral hemoglobin oxygenation during performance of a verbal fluency task in patients with alzheimer's disease monitored by means of near-infrared spectroscopy (nirs) – correlation with simultaneous rcbf-pet measurements. *Brain Research*, 755:293–303, 1997.

[44] Y. Hoshi. Functional near-infrared optical imaging: Utility and limitations in human brain mapping. *Psychophysiology*, 40:511–520, 2003.

[45] Y. Hoshi, S.-J. Chen, and M. Tamura. Spatiotemporal imaging of human brain activity by functional near-infrared spectroscopy. *American Laboratory*, pages 35–39, 2001.

[46] Y. Hoshi and M. Tamura. Detection of dynamic changes in cerebral oxygenation coupled to neuronal function during mental work in man. *Neuroscience Letters*, 150:5–8, 1993.

[47] Y. Hoshi and M. Tamura. Fluctuations in the cerebral oxygenation state during the resting period in functional mapping studies of the human brain. *Medical and Biological Engineering and Computing*, 35:328–330, 1997.

[48] K. Izzetoglu, S. Bunce, M. Izzetoglu, B. Onaral, and K. Pourrezaei. fnir spectroscopy as a measure of cognitive task load. In *Proceedings of the 25th Annual International Conference of the IEEE EMBS*, pages 3431–3434, 2003.

[49] K. Izzetoglu, S. Bunce, M. Izzetoglu, B. Onaral, and K. Pourrezaei. Functional near-infrared neuroimaging. In *Proceedings of the 26th Annual International Conference of the IEEE EMBS*, pages 5333–5336, 2004.

[50] K. Izzetoglu, G. Yurtsever, A. Bozkurt, and S. Bunce. Functional brain monitoring via nir based optical spectroscopy. In *Bioengineering Conference, 2003 IEEE 29th Annual, Proceedings of*, pages 335–336, 2003.

[51] K. Izzetoglu, G. Yurtsever, A. Bozkurt, B. Yazici, and S. Bunce. Nir spectroscopy measurements of cognitive load elicited by gkt and target categorization. In *Proceedings of 36th Hawaii International Conference on System Sciences*. IEEE, 2002.

[52] G. Jasdzewski, G. Strangman, J. Wagner, K. K. Kwong, R. A. Poldrack, and D. A. Boas. Differences in the hemodynamic response to event-related motor and visual paradigms as measured by near-infrared spectroscopy. *NeuroImage*, 20:479–488, 2003.

[53] F. F. Jobsis. Noninvasive, infrared monitoring of cerebral and myocardial oxygen sufficiency and circulatory parameters. *Science*, 198:1264–1267, 1977.

[54] O. Josephs, R. Turner, and K. Friston. Event related fmri. *Human Brain Mapping*, 5:243–248, 1997.

[55] R. Kennan, D. Kim, A. Maki, H. Koizumi, and R. T. Constable. Non-invasive assessment of language lateralization by transcranial near infrared optical topography and functional mri. *Human Brain Mapping*, 16:183–189, 2002.

[56] A. Kleinschmidt, H. Obrig, M. Requardt, K. D. Merboldt, U. Dirnagl, A. Villringer, and J. Frahm. Simultaneous recording of cerebral oxygenation changes during human brain activation by magnetic resonance imaging and near-infrared spectroscopy. *Journal of Cerebral Blood Flow and Matabolism*, 16:817–826, 1996.

[57] M. Kohl, C. Nolte, H. R. Heekeren, S. Horst, U. Scholz, H. Obrig, and A. Villringer. Changes in cytochrome-oxidase oxidation in the occipital cortex during visual stimulation: Improvement in sensitivity by the determination of the wavelength dependence of the differential pathlength factor. In *Proceedings of SPIE*, volume 3194, pages 18–27, 1998.

[58] M. Kohl, C. Nolte, H. R. Heekeren, S. Horst, U. Scholz, H. Obrig, and A. Villringer. Determination of the wavelength dependence of the differential pathlength factor from near-infrared pulse signals. *Physics in Medicine and Biology*, 43:1771–1782, 1998.

[59] M. H. Kutner, C. J. Nachtsheim, and J. Neter. *Applied Linear Regression Models*. McGraw-Hill Irwin, 4 edition, 2004.

[60] D. D. Langleben, L. Schroeder, J. A. Maldjian, R. C. Gur, S. McDonald, J. D. Ragland, C. P. O'Brien, and A. R. Childress. Brain activity during simulated deception: An event-related functional magnetic resonance study. *NeurImage*, 15:727–732, 2002.

[61] H. Liu, M. Miwa, B. Beauvoit, N. G. Wang, and B. Chance. Characterization of small-volume biological sample using time-resolved spectroscopy. *Anal. Biochem.*, 213:378–385, 1993.

[62] E. L. Maclin, K. A. Low, J. J. Sable, M. Fabiani, and G. Gratton. The event-related optical signal to electrical stimulation of the median nerve. *NeuroImage*, 21:1798–1804, 2004.

[63] S. J. Madsen, B. C. Wilson, M. S. Patterson, Y. D. Park, S. L. Jacques, and Y. Hefetz. Experimental tests of a simple diffusion model for the estimation of scattering and absorption coefficients of turbid media from time-resolved diffuse reflectance measurements. *Applied Optics*, 31:3509–3517, 1992.

[64] A. Maki, Y. Yamashita, Y. Ito, E. Watanabe, Y. Mayanagi, and H. Koizumi. Spatial and temporal analysis of human motor activity using noninvasive nir topography. *Journal of Neurosicence*, 11:1458–1469, 1995.

[65] A. Maki, Y. Yamashita, E. Watanabe, and H. Koizumi. Visualizing human motor activity by using non-invasive optical topography. *Front Med Biol Eng*, 7:285–297, 1996.

[66] D. Malonek and A. Grinvald. Interactions between electrical activity and cortical microcirculation revealed by imaging spectroscopy: Implications for functional brain mapping. *Science*, 272:551–554, 1996.

[67] J. Meek. Basic principles of optical imaging and application to the study of infant development. *Developmental Science*, 5(3):371–380, 2002.

[68] J. H. Meek, C. E. Elwell, M. J. Khan, J. Romaya, J. D. Wyatt, D. T. Delpy, and S. Zeki. Regional changes in cerebral hemodynamics as a result of a visual stimulus measured by near infrared spectroscopy. *Proceedings of Royal Society of London*, 261:351–356, 1995.

[69] J. H. Meek, M. Firbank, C. E. Elwell, J. Atkinson, O. Braddick, and J. S. Wyatt. Regional hemodynamic responses to visual stimulation in awake infants. *Pediatric Research*, 43:840–843, 1998.

[70] J. H. Meek, L. Tyszczuk, C. E. Elwell, and J. S. Wyatt. Cerebral blood flow increases over the first three days of life in extremely preterm neonates. *Archives of Disease in Childhood*, 78:F33–F37, 1998.

[71] J. H. Meek, L. Tyszczuk, C. E. Elwell, and J. S. Wyatt. Low cerebral blood flow is a risk factor for sever intraventricular hemorrhage. *Archives of Disease in Childhood*, 81:F15–F18, 1999.

[72] D. J. Mehagnoul-Schipper, B. F. van der Kallen, W. N. Colier, M. C. van der Sluijs, L. J. van Erning, H. O. Thijssen, B. Oeseburg, W. H. Hoefnagels, and R. W. Jansen. Simultaneous measurements of cerebral oxygenation changes during brain activation by near-infrared spectroscopy and functional magnetic resonance imaging in healthy young and elderly subjects. *Human Brain Mapping*, 16:14–23, 2002.

[73] M. Miwa, Y. Ueda, and B. Chance. Development of time-resolved spectroscopy system for quantitative non-invasive tissue measurement. *SPIE*, 2389:142–149, 1995.

[74] I. Miyai, H. Tanabe, I. Sase, H. Eda, I. Oda, I. Konishi, Y. Tsunazawa, T. Suzuki, T. Yanagida, and K. Kubota. Cortical mapping of gait in humans: A near-infrared spectroscopic topography study. *NeuroImage*, 14:1186–1192, 2001.

[75] Y. Noguchi, T. Takeuchi, and K. Sakai. Lateralized activation in the inferior frontal cortex during syntactic processing: event-related optical topography study. *Human Brain Mapping*, 17:89–99, 2002.

[76] Y. Nomura and M. Tamura. Quantitative analysis of hemoglobin oxygenation state of rat brain in vivo by picosecond time-resolved spectrophotometry. *Journal of Biochemistry*, 109:455–461, 1991.

[77] H. Obrig, M. Neufang, R. Wenzel, M. Kohl, J. Steinbrink, K. Einhaupl, and A. Villringer. Spontaneous low frequency oscillations of cerebral hemodynamics and metabolism in human adults. *NeuroImage*, 12:623–639, 2000.

[78] H. Obrig and A. Villringer. Beyond the visible–imaging the human brain with light. *Journal of Cerebral Blood Flow and Metabolism*, 23:1–18, 2003.

[79] H. Obrig, R. Wenzel, M. Kohl, S. Horst, P. Wobst, J. Steinbrink, F. Thomas, and A. Villringer. Near-infrared spectroscopy: does it function in functional activation studies of the adult brain? *International Journal of Psychophysiology*, 35:125–142, 2000.

[80] M. Oda, Y. Yamashita, G. Nishimura, and M. Tamura. Quantitation of absolute concentration change in scattering media by the time-resolved microscopic beer-lambert law. *Advances in Experimental and Medical Biology*, 345:861–870, 1992.

[81] M. Oda, Y. Yamashita, G. Nishimura, and M. Tamura. Determination of absolute concentration of oxy- and deoxyhemoglobin in rat head by time-resolved beer-lambert law. *SPIE*, 2389:770–778, 1995.

[82] M. Oda, Y. Yamashita, G. Nishimura, and M. Tamura. A simple and novel algorithm for time-resolved multiwavelength oximetry. *Physics in Medicine and Biology*, 41:955–961, 1996.

[83] E. Okada, M. Firbank, M. Schweiger, S. R. Arridge, M. Cope, and D. T. Delpy. Theoretical and experimental investigation of near infrared light propagation in a model of the adult head. *Applied Optics*, 36:21–31, 1997.

[84] N. Okui and E. Okada. Wavelength dependence of crosstalk in dual-wavelength measurement of oxy- and deoxy-hemoglobin. *Journal of Biomedical Optics*, 10(1):011015–1–011015–8, 2005.

[85] M. S. Patterson, B. Chance, and B. C. Wilson. Time resolved reflectance and transmittance for the non-invasive measurement of tissue optical properties. *Applied Optics*, 28(12):2331–2336, 1989.

[86] D. M. Rector, R. F. Rogers, J. S. Sschwaber, R. M. Harper, and J. S. George. Scattered-light imaging in vivo tracks fast and slow processes of neurophysiological activation. *NeuroImage*, 14:977–994, 2001.

[87] E. O. Reynolds, J. S. Wyatt, D. Azzopardi, D. T. Delpy, E. B. Cady, M. Cope, and S. Wray. New non-invasive methods for assessing brain oxygenation and hemodynamics. *British Medical Bulletin*, 44:1052–1075, 2004.

[88] K. Sakai, R. Hashimoto, and F. Homae. Sentence processing in the cerebral cortex. *Neuroscience Research*, 39:1–10, 2001.

[89] K. Sakatani, S. Chen, W. Lichty, H. Zuo, and Y. P. Wang. Cerebral blood oxygenation changes induced by auditory stimulation in newborn infants measure by near infrared spectroscopy. *Early Human Development*, 55:229–236, 1999.

[90] B. M. Salzberg and A. L. Obaid. Optical studies of the secretory event at vertebrate nerve terminals. *Experimental Biology*, 139:195–231, 1988.

[91] A. Sassaroli and S. Fantini. Comment on the modified beer-lambert law for scattering media. *Physics in Medicine and Biology*, 49:N255–N257, 2004.

[92] H. Sato, T. Takeuchi, and K. Sakai. Temporal cortex activation during speech recognition: an optical topography study. *Cognition*, 40:548–560, 1999.

[93] M. L. Schroeter, S. Zysset, T. Kupka, F. Kruggel, and D. Y. von Cramon. Near-infrared spectroscopy can detect brain activity during a color-word matching stroop task in an event-related design. *Human Brain Mapping*, 17(61):61–71, 2002.

[94] I.-Y. Son, M. Guhe, W. Gray, B. Yazici, and M. J. Schoelles. Human performance assessment using fnir. In *Proceedings of SPIE*, 2005.

[95] J. Steinbrink, M. Kohl, H. Obrig, G. Curio, F. Syre, F. Thomas, H. Wabnitz, H. Rinneberg, and A. Villringer. Somatosensory evoked fast optical intensity changes detected non-invasively in the adult human head. *Neuroscience Letters*, 291:105–108, 2000.

[96] J. Steinbrink, H. Wabnitz, H. Obrig, A. Villringer, and H. Rinneberg. Determining changes in nir absorption using layered model of the human head. *Physics in Medicine and Biology*, 46:879–896, 2001.

[97] R. A. Stepnowski, J. A. LaPorta, F. Raccuia-Behling, G. E. Blonder, R. E. Slusher, and D. Kleinfeld. Noninvasive detection of changes in membrane potential in cultured neurons by light scattering. *Proceedings of National Academy of Science USA*, 88:9382–9386, 1991.

[98] G. Strangman, D. A. Boas, and J. P. Sutton. Non-invasive neuroimaging using near-infrared light. *Biological Psychiatry*, 52:679–693, 2002.

[99] G. Strangman, J. P. Culver, J. H. Thompson, and D. A. Boas. A quantitative comparison of simultaneous bold fmri and nirs recordings during functional brain activation. *NeuroImage*, 17:719–731, 2002.

[100] T. Suto, M. Fukuda, M. Ito, T. Uehara, and M. Mikuni. Multichannel near-infrared spectroscopy in depression and schizophrenia: Cognitive brain activation study. *Biological Psychiatry*, 55:501–511, 2004.

[101] G. Taga, K. Asakawa, A. Maki, Y. Konishi, and H. Koizumi. Brain imaging in awake infants by near-infrared optical topography. *PNAS*, 100(19):10722–10727, 2003.

[102] Y. Takeuchi. Change in blood volume in the brain during a simulated aircraft landing task. *Journal of Occupational Health*, 42:60–65, 2000.

[103] I. Tasaki and P. M. Byrne. Rapid structural changes in nerve fibers evoked by electric current pulses. *Biochemical and Biophysical Research Communications*, 188:559–564, 1992.

[104] I. Tasaki and P. M. Byrne. Optical changes during nerve excitation: interpretation on the basis of rapid structural changes in the superficial gel layer of nerve fiber. *Physiological Chemistry and Physics and Medical NMR*, 26:101–110, 1994.

[105] V. Toronov, A. Webb, and J. H. Choi. Investigation of human brain hemodynamics by simultaneous near-infrared spectroscopy and functional magnetic resonance imaging. *Medical Physics*, 28(4):521–527, 2001.

[106] V. Toronov, A. Webb, J. H. Choi, M. Wolf, L. Safonova, U. Wolf, and E. Gratton. Study of local cerebral hemodynamics by frequency-domain near-infrared spectroscopy and correlation with simultaneously acquired functional magnetic resonance imaging. *Optics Express*, 9:417–427, 2001.

[107] K. Uludag, M. Kohl, J. Steinbrink, H. Obrig, and A. Villringer. Cross talk in the lambert-beer calculation for near-infrared wavelengths estimated by monte carlo simulations. *Journal of Biomedical Optics*, 7(1):51–59, 2002.

[108] A. Villringer and B. Chance. Non-invasive optical spectroscopy and imaging of human brain function. *Trends In Neurosciences*, 20(10):435–442, 1997.

[109] A. Villringer, J. Planck, C. Hock, L. Schleinkofer, and U. Dirnagl. Near infrared spectroscopy (nirs): a new tool to study hemodynamic changes during activation of brain function in human adults. *Neuroscience Letters*, 154:101–104, 1993.

[110] E. Watanabe, A. Maki, F. Kawaguchi, K. Takashiro, Y. Yamashita, H. Koizumi, and Y. Mayanagi. Non-invasive assessment of language dominance with near-infrared spectroscopic mapping. *Neuroscience Letters*, 256:49–52, 1998.

[111] E. Watanabe, Y. Yamashita, A. Maki, Y. Ito, and H. Koizumi. Noninvasive functional mapping with multi-channel near infrared spectroscopic topography in humans. *Neuroscience Letters*, 205:41–44, 1996.

[112] M. Wolf, U. Wolf, J. H. Choi, R. Gupta, L. P. Safonova, and L. A. Paunescu. Functional frequency-domain near-infrared spectroscopy detects fast neuronal signal in the motor cortex. *NeuroImage*, 17:1868–1875, 2002.

[113] Y. Yamashita, M. Oda, H. Naruse, and M. Tamura. In vivo measurement of reduced scattering and absorption coefficients of living tissue using time-resolved spectroscopy. *OSA TOPS*, 2:387–390, 1996.

[114] Y. Yamashita, M. Oda, E. Ohmae, and M. Tamura. Continuous measurement of oxy- and deoxyhemoglobin of piglet brain by time-resolved spectroscopy. *OSA TOPS*, 22:205–207, 1998.

[115]  P. Zaramella, F. Freato, A. Amigoni, s. Salvadori, P. Marangoni, A. Suppjei, B. Schiavo, and C. Lino. Brain auditory activation measured by near-infrared spectroscopy (nirs). *Pediatric Research*, 49:213–219, 2001.

[116]  Y. Zhang, D. H. Brooks, M. A. Franceschini, and D. A. Boas. Eigenvector-based spatial filtering for reduction of physiological interference in diffuse optical imaging. *Journal of Biomedical Optics*, 10:011014–1–011014–11, 2005.